

The dataset contains data for this study:

Elemental microanalyses.

Electrospray mass spectrum of *L* (plotted spectrum).

^1H and ^{13}C NMR spectra of *L* (raw and processed data).

X-ray Crystallographic data:

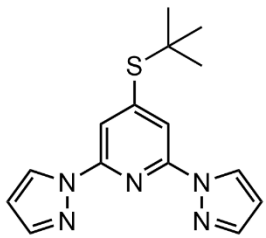
- Structure of α -*L* (CCDC 1991006).
- Structure of β -*L* (CCDC 1991007).
- Structure of $\mathbf{1}[\text{BF}_4]_2 \cdot x\text{CH}_3\text{NO}_2$ phase 1 at 120 K (CCDC 1991053).
- Structure of $\mathbf{1}[\text{BF}_4]_2 \cdot x\text{CH}_3\text{NO}_2$ phase 1 at 250 K (CCDC 1991052).
- Structure of $\mathbf{1}[\text{BF}_4]_2 \cdot x\text{CH}_3\text{NO}_2$ phase 3 at 120 K (CCDC 1991051).
- Structure of $\mathbf{1}[\text{BF}_4]_2 \cdot x\text{CH}_3\text{NO}_2$ phase 3 at 220 K (CCDC 1991050).
- Variable temperature unit cell data for $\mathbf{1}[\text{BF}_4]_2 \cdot x\text{CH}_3\text{NO}_2$ phase 3.
- Structure of $\mathbf{1}[\text{BF}_4]_2 \cdot \text{CH}_3\text{CN}$, monoclinic phase at 120 K (CCDC 1991049).
- Structure of $\mathbf{1}[\text{BF}_4]_2 \cdot \text{CH}_3\text{CN}$, monoclinic phase at 240 K (CCDC 1991048).
- Structure of $\mathbf{1}[\text{BF}_4]_2 \cdot \text{CH}_3\text{CN}$, monoclinic phase at 250 K (CCDC 1991047).
- Structure of $\mathbf{1}[\text{BF}_4]_2 \cdot \text{CH}_3\text{CN}$, monoclinic phase at 260 K (CCDC 1991046).
- Structure of $\mathbf{1}[\text{BF}_4]_2 \cdot \text{CH}_3\text{CN}$, monoclinic phase at 270 K (preliminary structure solution, not deposited with CCDC).
- Structure of $\mathbf{1}[\text{BF}_4]_2 \cdot \text{CH}_3\text{CN}$, triclinic phase (preliminary structure solution, not deposited with CCDC)
- Structure of $\mathbf{1}[\text{BF}_4]_2 \cdot y(\text{CH}_3)_2\text{CO}$ at 120 K (CCDC 1991045).
- Structure of $\mathbf{1}[\text{BF}_4]_2 \cdot y(\text{CH}_3)_2\text{CO}$ at 250 K (preliminary structure solution, not deposited with CCDC).
- Structure of $\mathbf{1}[\text{ClO}_4]_2 \cdot \text{CH}_3\text{NO}_2$ at 120 K (CCDC 1991044).
- Structure of $\mathbf{1}[\text{ClO}_4]_2 \cdot \text{CH}_3\text{NO}_2$ at 250 K (CCDC 1991043).
- Structure of $\mathbf{1}[\text{ClO}_4]_2 \cdot \text{CH}_3\text{NO}_2$ at 350 K (CCDC 1991042).
- Variable temperature unit cell data for $\mathbf{1}[\text{ClO}_4]_2 \cdot \text{CH}_3\text{NO}_2$.
- Structure of $\mathbf{1}[\text{ClO}_4]_2 \cdot \text{CH}_3\text{CN}$ at 120 K (CCDC 1991041).
- Structure of $\mathbf{1}[\text{ClO}_4]_2 \cdot \text{CH}_3\text{CN}$ at 180 K (CCDC 1991040).
- Structure of $\mathbf{1}[\text{ClO}_4]_2 \cdot \text{CH}_3\text{CN}$ at 230 K (CCDC 1991039).
- Structure of $\mathbf{1}[\text{ClO}_4]_2 \cdot \text{CH}_3\text{CN}$ at 250 K (CCDC 1991038).
- Structure of $\mathbf{1}[\text{ClO}_4]_2 \cdot \text{CH}_3\text{CN}$ at 290 K (CCDC 1991037).
- Structure of $\mathbf{1}[\text{ClO}_4]_2 \cdot \text{CH}_3\text{CN}$ at 330 K (CCDC 1991036).
- Variable temperature unit cell data for $\mathbf{1}[\text{ClO}_4]_2 \cdot \text{CH}_3\text{CN}$.
- Structure of $\mathbf{1}[\text{ClO}_4]_2 \cdot \frac{1}{2}(\text{CH}_3)_2\text{CO} \cdot 0.2\text{H}_2\text{O}$ at 120 K (CCDC 1991035).
- Structure of $\mathbf{1}[\text{ClO}_4]_2 \cdot \frac{1}{2}(\text{CH}_3)_2\text{CO} \cdot 0.2\text{H}_2\text{O}$ at 250 K (CCDC 1991034).
- Structure of $\mathbf{1}[\text{ClO}_4]_2$ (desolvated phase 2) at 120 K (CCDC 1991033).
- Structure of $\mathbf{1}[\text{ClO}_4]_2$ (desolvated phase 2) at 250 K (CCDC 1991032).

X-ray powder diffraction data (measured and simulated).

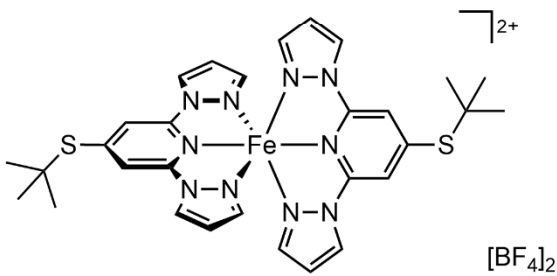
Thermogravimetric analyses (raw and plotted data).

Solid state magnetic susceptibility measurements (raw and processed data).

Compounds referred to in this dataset

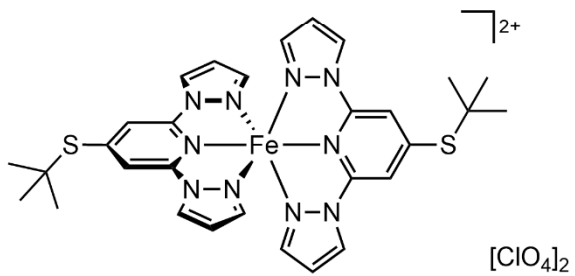


L
4-(*Tert*-butylsulfanyl)-2,6-di(pyrazol-1-yl)pyridine
 $C_{15}H_{17}N_5S$



$[FeL_2][BF_4]_2$
1 $[BF_4]_2$

Bis[4-(*tert*-butylsulfanyl)-2,6-di(pyrazol-1-yl)pyridine]-
iron(II) di(tetrafluoroborate)
 $C_{30}H_{34}B_2F_8FeN_{10}S_2$



$[FeL_2][ClO_4]_2$
1 $[ClO_4]_2$

Bis[4-(*tert*-butylsulfanyl)-2,6-di(pyrazol-1-yl)pyridine]-
iron(II) diperchlorate
 $C_{30}H_{34}Cl_2FeN_{10}O_8S_2$